PCCP

PAPER

View Article Online
View Journal | View Issue

Cite this: *Phys. Chem. Chem. Phys.*, 2024, **26**, 4759

Subphthalocyanine-flipper dyads for selective membrane staining†

José García-Calvo, *[abc] Xiao-Xiao Chen,[d] Naomi Sakai,[d] Stefan Matile [d] and Tomás Torres *[abc]

Received 10th November 2023,
Accepted 16th January 2024

DOI: 10.1039/d3cp05476d

rsc.li/pccp

The design, synthesis and evaluation of a subphthalocyanine-flipper (SubPc-Flipper) amphiphilic dyad is reported. This dyad combines two fluorophores that function in the visible region (420–800 nm) for the simultaneous sensing of both ordered and disordered lipidic membranes. The flipper probes part of the dyad possesses mechanosensitivity, long fluorescence lifetimes (τ = 3.5–5 ns) and selective staining of ordered membranes. On the other hand, subphthalocyanines (SubPc) are short-lifetime (τ = 1–2.5 ns) fluorophores that are insensitive to membrane tension. As a result of a Förster Resonance Energy Transfer (FRET) process, the dyad not only retains the mechanosensitivity of flippers but also demonstrates high selectivity and emission in different kinds of lipidic membranes. The dyad exhibits high emission and sensitivity to membrane tension ($\Delta\tau$ = 3.5 ns) when tested in giant unilamellar vesicles (GUVs) with different membrane orders. Overall, the results of this study represent a significant advancement in the applications of flippers and dyads in mechanobiology.

Introduction

Fluorescent dyads are powerful tools for photoluminescence studies. The presence of two fluorophores in close proximity allows the production of molecules with dual-tunable absorption/emission, enabling the control of fluorescence energy transfer (FRET) processes. As a result, dyads find applications in various fields, including chemical sensors,[1] double photon absorption processes[2] or super-resolution microscopy (SRM).[3] In particular, for biological applications, dyads offer numerous advantages when studying lipidic membranes. For instance, Anderson's group reported the use of a FRET-based dyad for SRM in vesicle membranes[4] and, more recently, the same group successfully developed a solvatochromic fluorescent dyad with a preference for the more disordered part of a vesicle membrane, when formed by a mixture of phospholipids.[5]

The objective of this study was to combine fluorescent flipper probes with subphthalocyanines (SubPcs) as an environment-insensitive complement, that is to synthesize and characterize the amphiphilic SubPc-Flipper **1** (Fig. 1). This dyad represents an opportunity to improve the design of membrane selective probes capable of distinguishing changes related parameters such as membrane tension,[6] polarity or water content and also retaining a high emission, independently of the membrane structure.

Fluorescent flippers are dithienothiophene dimers (DTT-$DTTO_2$) that provide the system with a donor/acceptor duality.[7] They exhibit a fascinating photochemical behavior involving possible planarization and increased conjugation when in the excited state.[8] Planarization only occurs in particular chemical environments and can be tuned by modifying the substituents of the flipper.[9,10] This process results in an environment sensitive red-shifted emission; affording operational mechanophores that have been repeatedly applied in chemical biology.[6,11] Consequently, derivatized flipper molecules have been utilized to stain and study the properties of different cellular membranes, with a linear correlation between fluorescence lifetimes and forces applied in the membrane.[12] In this regard, a series of derivatives have been synthesized, such as the Halo-flipper[13] for selective staining of organelles in modified cells, photocleavable-flippers[14] for studying the endocytosis pathway or the HydroFlipper[10,15] which serves as a starting point for this work.

HydroFlippers represent a new type of fluorescent flipper probes that are sensitive to both water and membrane tension. These compounds are characterized by having a trifluoroketone group, susceptible to hydration, in the terminal acceptor position (compound **2**, Fig. 1). Due to this substituent, flippers are not only mechanosensitive but they may hydrate in the presence of water, forming the twisted-hydrate (**th**, Fig. 1), which loses its fluorescent properties. Up to now, the advantages of the

[a] *Department of Organic Chemistry, Facultad de Ciencias, Universidad Autónoma de Madrid Cantoblanco, 28049-Madrid, Spain. E-mail: jose.garciac@uam.es*
[b] *Institute for Advanced Research in Chemical Sciences (IAdChem), Universidad Autónoma de Madrid, Campus de Cantoblanco, Madrid 28049, Spain*
[c] *IMDEA-Nanociencia, c/Faraday 9, Campus de Cantoblanco, Madrid 28049, Spain*
[d] *Department of Organic Chemistry, University of Geneva, Geneva, Switzerland*

† Electronic supplementary information (ESI) available: Detailed experiments, procedures and results are reported. See DOI: https://doi.org/10.1039/d3cp05476d

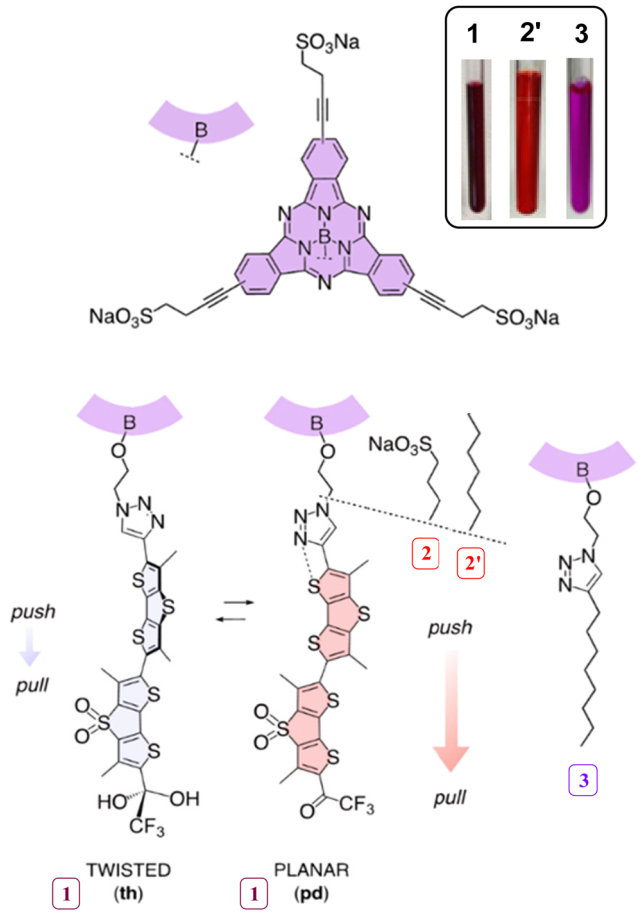

Fig. 1 Structure of dyad subphthalocyanine (SubPc) – Flipper **1** and their separate components, namely HydroFlipper **2** and SubPc **3**. Both dyad **1** and Hydroflipper **2** are dual-responsive twisted (**t**) and hydrated (**h**) probes that upon mechanical planarization (**p**) and chemical dehydration (**d**) in membranes of increasing order yield push–pull systems that red shift excitation and increase fluorescence intensity and lifetime. Environment-insensitive phthalocyanines with short lifetime are added to label disordered domains with high contrast and enhance ratiometric lifetime changes in response to tension. The picture in the right-up corner was taken from **1**, **2**′ and **3** dissolved in dry DMSO.

hydration were explored in two different ways, taking advantage of it as a dynamic equilibrium for super-resolution microscopy,[10] and using the probe as a dual reporter for the detection and differentiation of changes in membrane order *vs.* water content.[15]

Subphthalocyanines (SubPcs) are highly fluorescent molecules obtained from the cyclotrimerization of phthalonitriles in the presence of boron trihalides.[16] The scope of these aromatic conical shaped molecules entangles a broad variety of applications for all kind of photophysical[17] or supramolecular chemistry[18] studies, as well as applications in materials chemistry; such as OLEDs[19] or solar cells,[20] among many others. Thanks to the high fluorescence quantum yields and the many possible routes for derivatization, they can be also a potent tool in the field of chemical biology. Thus SubPcs have a remarkable performance in optical imaging and for photodynamic therapy.[21,22] Synthetically, SubPcs are mostly functionalized throughout two different approaches. On one side, the substituents of the periphery may be altered to change conjugation or add new functions, which modifies intermolecular interactions and photoluminescence properties. On the other hand, the axial substituent on the boron atom does not have a strong influence on the electronical properties, but it is used to introduce new functionalities or to control possible aggregation processes by changing the dipole moment of the molecule. Consequently, in the current case, the dyad was carefully designed to preserve the photoelectronic characteristics by introducing water-solubilizing groups at the periphery and the lipophilic flipper at axial position, which allows for the insertion in lipidic membranes and maintains the amphiphilic structure. Regarding the photophysical properties, SubPcs are particularly attractive because of their high molar extinction coefficients, as well as sharp peaks of absorption (570–580 nm) and emission (585–600 nm), with small Stokes shift, thus short lifetimes.[23] Moreover, their absorption and emission bands overlap with the respective bands of HydroFlippers (420–500 nm absorption, 590–750 nm emission), allowing their co-excitation and bidirectional FRET without undesired shifts. Therefore, the combination of SubPcs and HydroFlippers in dyads (such as **1**) was of interest to allow internal calibration, since the presence of the probe inside the membrane is clearly demonstrated, which complemented the environment-sensitive probe with varying fluorescence lifetime with an environment-insensitive probe of short lifetime.

The characteristics of SubPcs were of interest to label liquid-disordered (L_d) domains in multicomponent membranes and thus enhance the responsiveness for the following reasons. In fluorescence lifetime imaging microscopy (FLIM) of single-component membranes, fluorescent flippers report increasing membrane order from L_d to liquid-ordered (L_o) and solid-ordered (S_o) membranes with red shifts in excitation and increasing fluorescence intensity and lifetime (Fig. 2a). In FLIM images of multicomponent membranes, fluorescent flippers report increasing membrane tension as an increase in fluorescent lifetime. This response originates from tension-induced assembly of highly ordered microdomains with long-lived, highly emissive, planarized flippers (Fig. 2b). In reverse, decreasing tension decreases lifetimes because of tension-induced disassembly of microdomains with long-lived flippers (Fig. 2b). This responsiveness to tension changes is limited by the poor fluorescence intensity of short-lived twisted flippers in L_d membranes. Without contrasting emission from L_d membranes, disassembly of ordered microdomains with decreasing tension will be recorded as decreasing intensity, that is decreasing counts in FLIM histograms for long-lived planarized flippers rather than as a decrease in fluorescent lifetime. Although less significant because of overall poor intensity, it can be added that planarization of flippers in L_d domains upon lipid compression by decreasing tension increases rather than decreases lifetimes, which weakens rather than enhances the dominant response of flipper deplanarization from tension-induced domain disassembly. In HydroFlipper **2**, the emission from twisted flippers **2th** in L_d membranes is further weakened by hydration (Fig. 1). With SubPc-Flipper **1th** in L_d membranes, fluorescent properties should thus be dominated by the short-lived, highly-emissive and tension-insensitive SubPc (Fig. 2c, purple). In L_o membranes, the

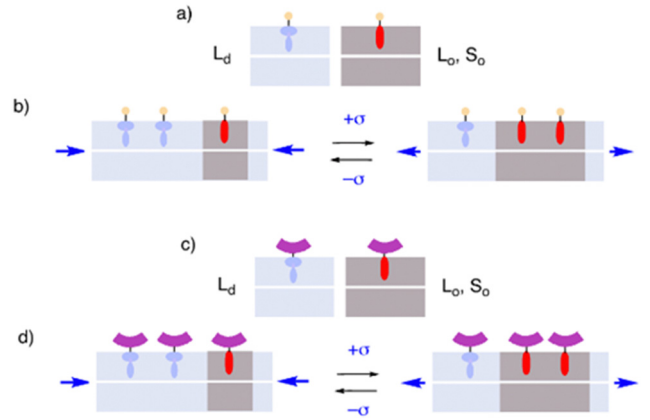

Fig. 2 (a) Mechanical flipper planarization reports increasing membrane order with red shifts and increasing intensity and lifetime. (b) Responsiveness to tension-induced domain dis/assembly is limited by insufficient short-lifetime emission from L_d domains. (c) SubPc-Flippers add tension-insensitive high-intensity short-lifetime emission to (d) label L_d domains and provide contrast to increasing emission of planar flippers in growing L_o domains with increasing tension.

fluorescence properties of SubPc-Flipper **1pd** should be dominated by the long-lived, tension-sensitive flipper (Fig. 2c, red).

In multicomponent membranes, the response to high tension with many ordered microdomains should be dominated by the long-lived, tension-sensitive flipper (Fig. 2d, red). While HydroFlipper **2** turns off fluorescence, the response of SubPc-Flipper **1** to low tension with a few ordered domains should be dominated by the short-lived, tension-insensitive SubPc (Fig. 2d, purple). As a result, SubPc-Flipper **1** should label L_d domains at low lifetime with high contrast, which in turn should increase the responsiveness of the small-molecule fluorescent probe to changes in membrane tension.

Results and discussion

Synthesis

With the idea of the amphiphilic SubPc-Flipper **1** in mind, five derivatives were synthesized (compounds **2** and **2′** from Fig. 1 and **1**, **3** and **4** from Scheme 1). First, following a reported procedure, HydroFlippers **2** and **2′** were synthesized. On the other hand, the amphiphilic SubPc **3** was also prepared, with an analogous structure to **1** but with an aliphatic octyl-chain instead of the flipper. Finally, a SubPc-flipper soluble in organic solvents (**4**) was also synthetized.

The synthesis involved two convergent routes for flipper and SubPc. For flippers **11**, **2** and **2′**, the reported route was followed.[10] On the other hand, the synthesis of SubPc started with the previously reported triiodo-SubPc **5**.[24] The first step involved the reaction of the chloride in the axial position with 2-hydroxyethyl-1-azide through nucleophilic substitution in toluene and in the presence of base, resulting in the formation of SubPc **6**.[25] After purification and characterization, compound **6** underwent click chemistry conditions using $CuSO_4$ and sodium ascorbate in dichloromethane. Flipper **11** was derivatized into **7**

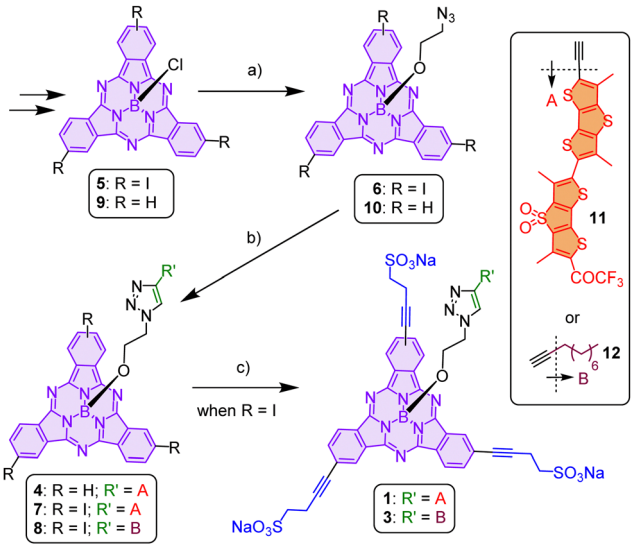

Scheme 1 When R = I: (a) 2-hydroxyethyl-1-azide, DBU, toluene, 84%; if R′ = **A** (b) **11**, $CuSO_4{\cdot}5H_2O$, sodium ascorbate, CH_2Cl_2:THF:H_2O, rt, 12 h, 42% and (c) but-3-yne-1-sulfonate, $PdCl_2(PPh_3)_2$, CuI, Et_3N, THF, rt, 48 h, 19%; if R′ = B (b) **12**, 1-decyne, $CuSO_4{\cdot}5H_2O$, sodium ascorbate, CH_2Cl_2:H_2O, rt, 2 h, 79%; (c) but-3-yne-1-sulfonate, $PdCl_2(PPh_3)_2$, CuI, Et_3N, THF, rt, 36 h, 27%. When R = H: (a) 2-hydroxyethyl-1-azide, DBU, toluene, 80%; (b) $CuSO_4{\cdot}5H_2O$, sodium ascorbate, CH_2Cl_2:H_2O, rt, 12 h, 29%.

while with 1-decyne **12**, SubPc **8** was obtained. Next, to make compounds **7** and **8** amphiphilic, 4-sufonate-but-1-yne was introduced throughout a triple Sonogashira coupling at the periphery of the SubPc, resulting in the formation of compounds **1** and **3**, respectively. Additionally, a non-amphiphilic derivative, the dyad SubPc-Flipper **4**, was also synthesized. To obtain dyad **4**, a synthetically equivalent route was followed, where the azide derivative **10** was first synthesized and then, through click chemistry, dyad **4** was obtained. For further details about the synthesis and characterization, please refer to Section 2 of the ESI.†

Spectroscopical properties in solution

First, it must be taken into account that for SubPc **3** there was no significant changes in absorption or fluorescence depending on the solvent, but that was not the case for dyad **1**. As it was reported for Flipper **2**, and explained in the introduction, dyad **1** showed a duality between the planarized ketone (**pd**) and the twisted hydrate (**th**) (see Fig. 1). The equilibrium (pd-th) results in a blue shifted absorption/emission whenever in the hydrated form. However, amphiphiles such as **1** and **3** possess low solubility in aprotic or low-polarity solvents. Therefore, and being limited to the solubility of the amphiphiles, the photoluminescence of **1** in solution was mostly associated to the hydrate **1th** (or hemiacetal in methanol solutions). For that reason, the results are also compared to the corresponding non-amphiphilic equivalents of the SubPc-Flipper **1** (**4**) and HydroFlipper **2** (**2′**); which provided a better understanding of the dyad behaviour, not only in solution but also in the following studies in phospholipid membranes (*vide infra*).

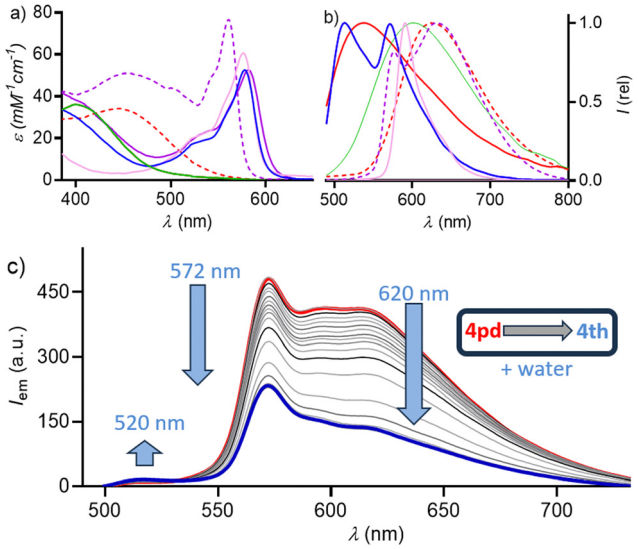

Fig. 3 (a) ε *vs.* λ and (b) normalized emission spectra of **1** (plain blue, CH_3OH), **2** (plain green CH_3OH), **2′** (dashed red, dioxane; plain red water/dioxane 1 : 25), **3** (pink, CH_3OH), **4** (dashed purple, $CHCl_3$; plain purple, CH_3OH). (c) Emission intensity profile of **4** in dioxane after adding 1.5% of water (30 min, red to blue); for more details see Section S5 of the ESI.†

The amphiphilic control **3** in methanol showed a sharp absorption at 577 nm (Q-band) and an emission peak at 590 nm (Fig. 3a and b, pink). Additionally, changing solvents had no significant impact on the Stokes shifts (Fig. S2b, ESI†), as it is generally reported for SubPcs.[26] Conversely, the equilibria in HydroFlipper **2′pd** (dioxane) to **2′th** (water:dioxane, 1 : 25 water) produced a blue shift in the absorption band from 446 nm to 400 nm and in fluorescent emission from 619 to 537 nm (Fig. 3a and b, red). In presence of protic solvents, such as methanol or water, **1** and **4** presented an absorption band around 400 nm, associated to the forms **1th** and **4th** (Fig. 3a, blue and plain purple), confirming the same behaviour than for their HydroFlipper equivalents (**2** and **2′**). Still, in aprotic solvents, such as chloroform, dyad **4** (Fig. 3a, dashed purple) showed red shifted flipper absorption/emission (**4pd**), as it was the case for **2′** (Fig. 3a, dashed red). Besides, molar extinctions coefficients (ε) for dyads **1** (λ_{578}, MeOH, 53 ± 3 mM^{-1} cm^{-1}) and **4** (λ_{561} ($CHCl_3$) = 63 ± 3 mM^{-1} cm^{-1}, λ_{582} (MeOH) = 56 ± 3 mM^{-1} cm^{-1}), were also matching to a theoretical sum of the components, SubPc **3** (λ_{577}, MeOH, 61 ± 4 mM^{-1} cm^{-1}) and Flipper **2′** (λ_{446}, dioxane, 34 ± 2 mM^{-1} cm^{-1}, λ_{399}, water/dioxane, 30 ± 2 mM^{-1} cm^{-1}) or **2** (λ_{399}, MeOH, 36 ± 4 mM^{-1} cm^{-1}).

Furthermore, **4** exhibited an environment dependent FRET response (see Fig. 3b, purple; and Fig. S4 and S5 from the ESI†). In aprotic solvents, two emission bands were observed, corresponding to the SubPc (≈570 nm) and HydroFlipper (600–700 nm), partially overlapping and showing a FRET from the HydroFlipper probe to the SubPc. Here, low fluorescence quantum yields (ϕ_F) were found for dyad **1th** (2%, CH_3OH) and **4th** (2%, diox:water), which contrasted with dyad **4** in aprotic solutions (**4pd**, $CHCl_3$, 17%) and SubPc **3** (14%, MeOH). As it was reported before, the equilibrium (pd-th) produced a decrease in the fluorescent quantum yield (ϕ_F) from **2′pd** from 27% (dioxane) to **2′th** 2% (water:dioxane, 4% water). Although a lower fluorescent emission was expected for **1th** and **4th**, the remaining SubPc emission went below the reported for the control **3**, whose value is typical for other reported SubPcs.[16] The lower emission of **1th** and **4th** may be explained by the orientation of the dipoles in protic solvents that produces a quenching by FRET from the SubPc to the low-emitting hydrated flippers. The fluorescence quenching is most noticeable when adding water to aprotic solutions (Fig. 3c) or in studies in membranes (*vide infra*) agreeing with the proposed explanation and results from other fluorescent dyads.[5]

Time dependent hydration studies were also performed, demonstrating the change from ketone form **4pd** to the hydrate **4th**. Dyad **4** showed a decrease in emission when water is added (Fig. 3c). It came together with a disappearance of the emission coming from the flipper and takes place in less than 30 min after adding 1.5% of water to a dioxane solution at room temperature. This is further corroborated by a small increase in the emission at 520 nm, with much lower intensity, and associated to the emission of DTT components of the flipper separately (see Fig. S6 for a comparison of the change in fluorescence at 520/620 nm, ESI†).

Fluorescence spectroscopy with LUVs

In order to compare the response to membrane tension, similar vesicle experiments to previous publications were performed.[8] The amphiphilic SubPc control **3** showed the characteristic spectra with a sharp excitation maximum at 582 nm and a nearly mirror imaged emission maximizing at 592 nm (Fig. 4a). Both excitation and emission spectra were insensitive to the environment of the SubPc fluorophore. Spectra of **3** in buffer without and with LUVs composed of L_d DOPC (1,2-dioleoyl-*sn*-glycero-3-phosphocholine) and L_o SM/CL (egg sphingomyelin/cholesterol) 7 : 3 were nearly superimposable.

The fluorescence spectra of HydroFlipper **2** were as reported previously.[10,15] Namely, fluorescence was completely quenched in buffer, possibly due to self-assembly of the amphiphiles into micelles. Also in L_d LUVs, fluorescence was negligible because twisting and hydration into **2th** both decrease fluorescence intensity (Fig. 4c, gold). In L_o LUVs, **2** was highly fluorescent. The red-shifted excitation band showed vibrational finestructure with a 0–0 transition at 560 nm, and the emission maximum at 624 nm (Fig. 4c, green). Both red shift and increasing intensity were consistent with dehydration and mechanical compression of twisted **2th** into planar conformer **2pd** (Fig. 1 and 2).

SubPc-Flipper **1** in water was essentially not fluorescent. This contrast to SubPc-control **3** could imply FRET from SubPc to the non-emissive flippers under these conditions, or direct self-quenching of self-assembled SubPc in micelles (Fig. 4b, blue). The spectra of **1** in L_d LUVs were dominated by contributions from SubPc (Fig. 4b, gold). The absence of flippers' contribution in the emission spectra could be rationalized by its very weak emission in L_d membranes. On the other hand, the excitation spectra contained contributions from flippers, indicating the efficient FRET from flippers to SubPc. Compared to SubPc-control **3**, the emission of **1** was weaker, probably due

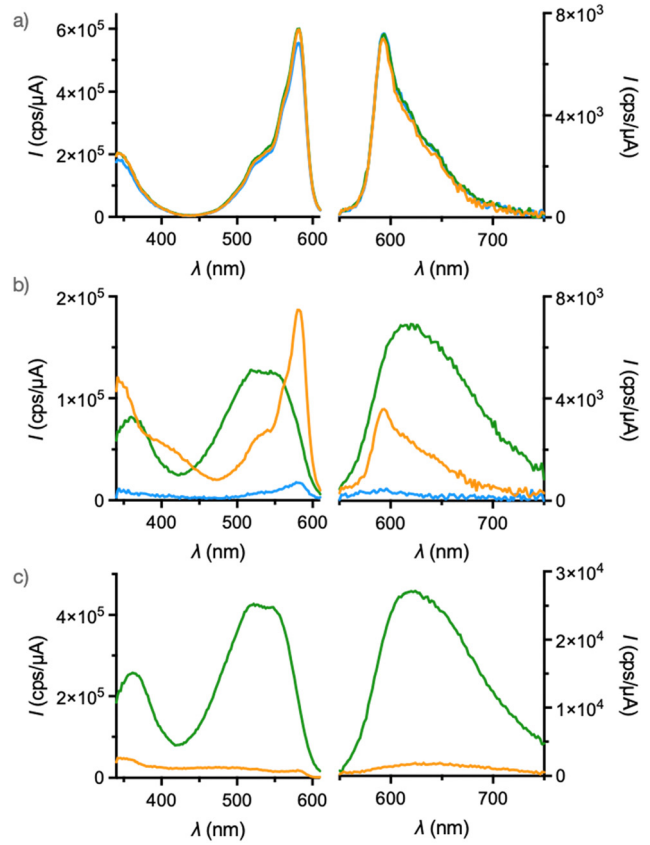

Fig. 4 Excitation (left, λ_{em} = 650 nm) and emission spectra (right, λ_{ex} = 480 nm) of **3** (a, 150 nM), **1** (b, 120 nM), and **2** (c, 100 nM) in SM/CL (7 : 3, green) or DOPC LUVs (gold), and buffer (blue) at 25 °C.

to FRET from SubPc to the less fluorescent flippers. However, SubPc quenching was much less pronounced in L_d LUVs than in buffer, suggesting that the two fluorophores are well separated and orthogonally oriented also in L_d LUVs. Such nearly perpendicular orientation of transition dipoles should result in less efficient FRET. This interpretation was consistent with the results obtained in solution and with fluorescence anisotropy in GUVs, described later on.

In sharp contrast, the spectra of **1** in L_o LUVs were dominated by the known characteristics of planarized flippers **2pd**, with wide, slightly fine-structured excitation maxima from 500–550 nm, and broad emission maxima from 600–650 nm (Fig. 4b, green). Within these broad bands, the sharp SubPc maxima were almost invisible, only as a bathochromic shoulder of the excitation band (Fig. S8, ESI†). The identically shaped emission spectra were also obtained upon excitation at 560 nm where the absorbance of SubPc is higher, indicating a significant FRET from SubPc to planarized flippers (Fig. S7, ESI†). Fluorescence was overall weaker than **2** in L_o membrane, due probably to flippers to SubPc FRET and/or the inner filter effect.

Taken together, fluorescence spectroscopy of **1** in LUVs reported on L_d and L_o membranes with similarly high intensities and distinct signatures (Fig. 4b, green *vs.* gold). With SubPc-free flippers like **2**, such iso-emissive labeling of membranes of different order is not possible because of insufficient intensity at high disorder (Fig. 4c, green *vs.* gold).

Fluorescence lifetime imaging microscopy with GUVs

FLIM images of SubPc-Flipper **1** in multi-component GUVs showed labeling of L_d and L_o domains with high intensity and high contrast (Fig. 5d). The colorful images were in stark contrast to the FLIM images of HydroFlipper **2**, which labeled L_o domains almost exclusively (Fig. 5g).

The average lifetime τ_{av} = 4.9 ns of **1** in L_o domains was as long as for other flippers in planar conformation (Table 1). Nevertheless, the average lifetime τ_{av} = 1.3 ns in the bright blue L_d domains was exceptionally short (Fig. 5d, f and Table 1). It was much shorter than τ_{av} = 1.9 ns for control **3** (Fig. 5a and Table 1). This additional lifetime shortening was likely to originate from FRET from SubPc to flippers, as already observed in LUVs (Fig. 4b).

The lifetime τ_{av} = 1.3 ns of **1** in the bright blue L_d domains in multicomponent GUVs was also much shorter than the τ_{av} = 2.2 ns of pale green L_d domains in multicomponent GUVs labeled with HydroFlipper **2** (Fig. 4d and g and Table 1). The difference $\Delta\tau_{L_d\text{-}L_o}$ = 2.5 ns between L_o and L_d domains labeled with **2** increased to a record $\Delta\tau_{L_d\text{-}L_o}$ = 3.2 ns for **1**. At comparable intensity, this difference $\Delta\tau_{L_d\text{-}L_o}$ should correlate directly with responsiveness to changes in membrane tension.

The total lifetime τ_{mix} = 4.0 ns of HydroFlipper **2** in multicomponent GUVs was near the τ_{L_o} = 4.7 ns of the L_o domains (Table 1). This similarity was as expected from the poor fluorescence of twisted **2th** in L_d domains (Fig. 5g). In contrast, the total lifetime τ_{mix} = 1.4 ns of **1** in multicomponent GUVs was nearer to the τ_{L_d} = 1.3 ns in L_d than the τ_{L_o} = 4.5 ns in L_o

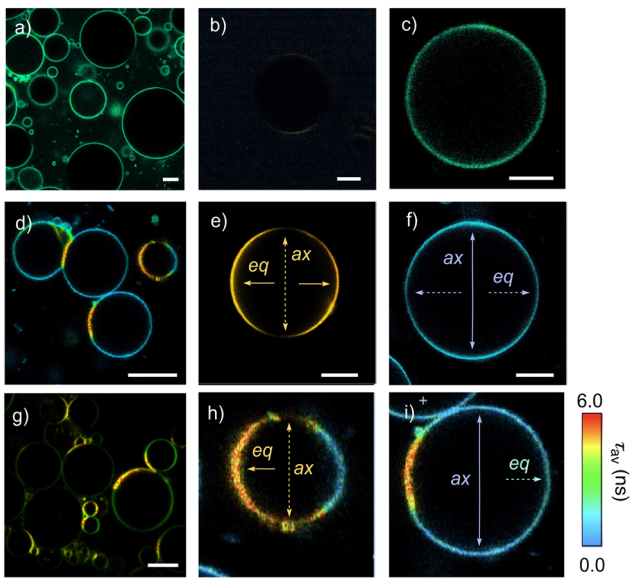

Fig. 5 FLIM images of **3** (a)–(c), **1** (d)–(f) and **2** (g) in GUVs composed of DOPC/SM/CL 3 : 2 : 1 (a), (d) and (g), SM/CL 7 : 3 (b), (e) and DOPC (c) and (f) with enlarged parts of (d) to indicate orthogonal anisotropy (h, i, eq = equatorial, ax = axial). Scale bars = 10 μm, time bar = 0–6 ns, laser at 530 nm.

Table 1 Fluorescence lifetime data[a] for SubPc-flippers **1** and controls in L_d, L_o and mixed GUVs and cells[b]

P[c]	τ_{L_d}[d]	τ_{L_o}[e]	$\Delta\tau_{L_d\text{-}L_o}$[f]	τ_{mix}[g]	τ_{iso}[h]
1	1.4/1.3	4.9/4.5	3.5/3.2	1.4	3.7
2[i]	2.1/2.2	4.7/4.7	2.6/2.5	4.0	4.6
3	1.9/1.9	—	—	1.9	—

[a] Fitting uncertainty ± 0.2 ns. [b] Intensity averaged lifetimes (τ_{av}) in ns. [c] Probes (Fig. 1). [d] Lifetime τ_{av} in FLIM images of single-component L_d GUVs (DOPC)/L_d domains (τ_2) of multicomponent GUVs. [e] Lifetime τ_{av} in FLIM images of single-component L_o GUVs (SM/CL 7 : 3)/L_o domains (τ_3) of multicomponent GUVs. [f] Lifetime difference between FLIM images of single-component L_o and L_d GUVs/domains in multicomponent GUVs. [g] Lifetime τ_{av} in FLIM images of multi-component GUVs with L_o and L_d domains (DOPC/SM/CL 3 : 2 : 1). [h] Lifetime τ_{av} of the plasma membrane in FLIM images of HK cells. [i] Data are from ref. 8 except for those of multicomponent GUVs.

domains (Table 1). The total lifetime obviously depends on the partitioning preference of the probes in different domains, and their areas, which are different from measurement to measurement. Nevertheless, compared to **2** much shorter τ_{mix} = 1.4 ns is unattainable without high intensity and short lifetime of SubPc enhancers added in the L_d domains (Fig. 4d). Taken together, the environment-insensitive SubPc enhancer in dyad **1** labels L_d domains in multicomponent membranes with high intensity and short lifetime, which lowers the total lifetime in multicomponent GUVs from τ_{mix} = 4.0 ns to τ_{mix} = 1.4 ns and increases the lifetime difference between L_d and L_o domains from $\Delta\tau_{L_d\text{-}L_o}$ = 2.5 to $\Delta\tau_{L_d\text{-}L_o}$ = 3.2 ns. These are significant differences that should correlate with the responsiveness of membrane tension in living cells. However, these measurements were not possible because in HeLa Kyoto (HK) cells, SubPc-Flipper **1** was internalized partially under isoosmotic and fully under hyperosmotic conditions (Fig. S11, ESI†). However, reduced lifetimes τ_{iso} = 3.7 ns of **1** in the plasma membrane only of HK cells compared to τ_{iso} = 4.6 ns of **2** were consistent with increased contributions from tension-insensitive enhancers in L_d domains and thus increased responsiveness to changes in membrane tension (Table 1). We also note that molecular design strategies to prevent probe internalization exist.

In single-component L_o GUVs, FLIM images of SubPc-Flipper **1** showed strong anisotropy with bright equatorial and dark axial regions (Fig. 5e). This anisotropy originates from the selective excitation of fluorophores oriented parallel to the polarized light, is characteristic for flipper probes in ordered membranes and consistent with tight alignment of the probes along the uniformly oriented tails of one leaflet.

In single-component L_d GUVs, FLIM images of **1** showed orthogonal anisotropy with brighter axial than equatorial regions (Fig. 5f). Originating from short-lived SubPc emission, this orthogonal anisotropy suggested that the orientation of SubPc enhancers and flippers is perpendicular to each other. With the hydrophobic flippers oriented along the lipid tails, orthogonal anisotropy aligns the trianionic SubPcs parallel with the membrane water interface (Fig. 2). The detectability of this orthogonal SubPc anisotropy was remarkable considering that in disordered membranes, flipper alignment along less constrained lipid tails is insufficient to produce significant anisotropy. It suggested that the three peripheral sulfonate anions probably all ion pair with ammonium cations in the plane of the membrane surface to ensure sufficient alignment.

In multicomponent GUVs, the anisotropy of planarized flippers in ordered domains was preserved (Fig. 5h). The failure of SubPc to color the dark axial regions in blue was consistent with efficient SubPc quenching by intramolecular FRET to flippers under these conditions, as observed already during spectroscopic analysis in LUVs or in solution. The orthogonal anisotropy of SubPc in disordered domains was also preserved in multicomponent GUVs (Fig. 5i). However, the equator regions were not darkened but colored pale green (Fig. 5i). This small increase in lifetime indicated that emission from twisted flippers compensates for orthogonal SubPc anisotropy. This behavior in L_d domains (Fig. 5i) was contrary to lacking anisotropy compensation in single-component L_d membranes (Fig. 4i) and L_o domains (Fig. 4h). It suggested that in multicomponent GUVs, flipper quenching by FRET to SubPc in L_d domains is less effective than SubPc quenching by FRET to flippers in L_d as well as L_o domains.

Conclusions

The combination of SubPc-flipper was successfully achieved, developing a new tool for staining multicomponent lipidic membranes. The photoluminescence properties of SubPc-Flipper were studied in solution, vesicle membranes, and HK cells. It has been demonstrated that in highly ordered membranes (L_o), the flipper's long fluorescence lifetimes are detected, while in highly disordered membranes (L_d), the SubPc's fluorescence lifetime is predominant. This selective labeling offers a better understanding of the partition between ordered and disordered phases in lipidic membranes.

This advancement represents progress in employing dyads for fluorescence staining of membranes. It complements information from each individual reporter and has potential applications for improved selective cell membrane staining. Therefore, it is demonstrated that the use of multicomponent probes may lead to a deeper understanding of membranes providing highly attractive possibilities for chemical biology.

Author contributions

J. G-C.: conceptualization, synthesis, characterization, measurements in solution, interpretation of results and MS + SI writing. X-X. C.: vesicle and cell experiments, data treatment and interpretation and SI writing. N. S.: vesicle and cell experiments, data treatment and interpretation, MS and SI writing. S. M.: conceptualization, interpretation, resources and MS writing. T. T. conceptualization, resources, supervision and MS writing.

Conflicts of interest

The University of Geneva has licensed Flipper-TR® probes to Spirochrome for commercialization.

Acknowledgements

We thank the NMR, MS and Bioimaging platforms for services, and the University of Geneva, the National Centre of Competence in Research (NCCR) Chemical Biology (51NF40-185898), the NCCR Molecular Systems Engineering (51NF40-182895), as well as the Swiss NSF for financial support (Excellence Grant 200020 204175; Swiss-ERC Advanced Grant TIMEUP, TMAG-2_209190). J. G. C. acknowledges his funding from ''Ayudas María Zambrano para la atracción de talento internacional'' (CA3/RSUE/2021-00243) from the Spanish Government/EU funds at Universidad Autónoma de Madrid, and ''Ayudas de atracción de talento de la Comunidad de Madrid 2022'' (2022-T1/IND-23907) supported by Comunidad de Madrid with EU funds at IMDEA Nanociencia. T. T. acknowledges financial support from the Spanish AEI/MICINN (PID2020-116490GB-I00) and the Comunidad de Madrid and the Spanish State through the Recovery, Transformation and Resilience Plan [''Materiales Disruptivos Bidimensionales (2D)'' (MAD2D-CM) (UAM1)-MRR Materiales Avanzados], and the European Union through the Next Generation EU funds. IMDEA Nanociencia acknowledges support from the ''Severo Ochoa'' Programme for Centres of Excellence in R&D (MINECO, Grant SEV2016-0686).

Notes and references

1 A. Vanessa Saura, M. Isabel Burguete, F. Galindo and S. V. Luis, *Org. Biomol. Chem.*, 2017, **15**, 3013–3024.
2 D. Collado, P. Remón, Y. Vida, F. Najera, P. Sen, U. Pischel and E. Perez-Inestrosa, *Chem. – Asian J.*, 2014, **9**, 797–804.
3 E. Deniz, S. Ray, M. Tomasulo, S. Impellizzeri, S. Sortino and F. M. Raymo, *J. Phys. Chem. A*, 2010, **114**, 11567–11575.
4 A. T. Frawley, V. Wycisk, Y. Xiong, S. Galiani, E. Sezgin, I. Urbančič, A. Vargas Jentzsch, K. G. Leslie, C. Eggeling and H. L. Anderson, *Chem. Sci.*, 2020, **11**, 8955–8960.
5 A. T. Frawley, K. G. Leslie, V. Wycisk, S. Galiani, D. Shrestha, C. Eggeling and H. L. Anderson, *Chem. Phys. Chem.*, 2023, **24**, e202300125.
6 A. Colom, E. Derivery, S. Soleimanpour, C. Tomba, M. D. Molin, N. Sakai, M. González-Gaitán, S. Matile and A. Roux, *Nat. Chem.*, 2018, **10**, 1118–1125.
7 J. García-Calvo, J. López-Andarias, N. Sakai and S. Matile, *Chem. Commun.*, 2021, **57**, 3913–3916.
8 M. Dal Molin, Q. Verolet, A. Colom, R. Letrun, E. Derivery, M. Gonzalez-Gaitan, E. Vauthey, A. Roux, N. Sakai and S. Matile, *J. Am. Chem. Soc.*, 2015, **137**, 568–571.
9 J. García-Calvo, J. López-Andarias, N. Sakai and S. Matile, *Helv. Chim. Acta*, 2022, **105**, e202100238.
10 J. García-Calvo, J. Maillard, I. Fureraj, K. Strakova, A. Colom, V. Mercier, A. Roux, E. Vauthey, N. Sakai, A. Fürstenberg and S. Matile, *J. Am. Chem. Soc.*, 2020, **142**, 12034–12038.
11 C. Roffay, G. Molinard, K. Kim, M. Urbanska, V. Andrade, V. Barbarasa, P. Nowak, V. Mercier, J. García-Calvo, S. Matile, R. Loewith, A. Echard, J. Guck, M. Lenz and A. Roux, *Proc. Natl. Acad. Sci. U. S. A.*, 2021, **118**, e2103228118.
12 A. Goujon, A. Colom, K. Straková, V. Mercier, D. Mahecic, S. Manley, N. Sakai, A. Roux and S. Matile, *J. Am. Chem. Soc.*, 2019, **141**, 3380–3384.
13 K. Straková, J. López-Andarias, N. Jiménez-Rojo, J. E. Chambers, S. J. Marciniak, H. Riezman, N. Sakai and S. Matile, *ACS Cent. Sci.*, 2020, **6**, 1376–1385.
14 J. López-Andarias, K. Straková, R. Martinent, N. Jiménez-Rojo, H. Riezman, N. Sakai and S. Matile, *JACS Au*, 2021, **1**, 221–232.
15 J. García-Calvo, J. López-Andarias, J. Maillard, V. Mercier, C. Roffay, A. Roux, A. Fürstenberg, N. Sakai and S. Matile, *Chem. Sci.*, 2022, **13**, 2086–2093.
16 G. Lavarda, J. Labella, M. V. Martínez-Díaz, M. S. Rodríguez-Morgade, A. Osuka and T. Torres, *Chem. Soc. Rev.*, 2022, **51**, 9482–9619.
17 H. Gotfredsen, D. Thiel, P. M. Greißel, L. Chen, M. Krug, I. Papadopoulos, M. J. Ferguson, M. B. Nielsen, T. Torres, T. Clark, D. M. Guldi and R. R. Tykwinski, *J. Am. Chem. Soc.*, 2023, **145**, 9548–9563.
18 J. Labella, G. Lavarda, L. Hernández-López, F. Aguilar-Galindo, S. Díaz-Tendero, J. Lobo-Checa and T. Torres, *J. Am. Chem. Soc.*, 2022, **144**, 16579–16587.
19 N. F. Farac, A. R. Tetreault and T. P. Bender, *J. Phys. Chem. C*, 2023, **127**, 702–727.
20 H. Gotfredsen, T. Neumann, F. E. Storm, A. V. Muñoz, M. Jevric, O. Hammerich, K. V. Mikkelsen, M. Freitag, G. Boschloo and M. B. Nielsen, *ChemPhotoChem*, 2018, **2**, 976–985.
21 N. M. Casellas, G. Dai, E. Y. Xue, A. Fonseca, D. K. P. Ng, M. García-Iglesias and T. Torres, *Chem. Commun.*, 2022, **58**, 669–672.
22 E. Winckel, M. Mascaraque, A. Zamarrón, Á. Juarranz De La Fuente, T. Torres and A. Escosura, *Adv. Funct. Mater.*, 2018, **28**, 1705938.
23 I. D. Burtsev, T. V. Dubinina, A. E. Egorov, A. A. Kostyukov, A. V. Shibaeva, A. S. Agranat, M. M. Ivanova, L. R. Sizov, N. V. Filatova, A. Y. Rybkin, E. V. Varakina, A. S. Bunev, A. A. Antonets, E. R. Milaeva and V. A. Kuzmin, *Dyes Pigm.*, 2022, **207**, 110690.
24 D. González-Rodríguez, T. Torres, M. Á. Herranz, L. Echegoyen, E. Carbonell and D. M. Guldi, *Chem. – Eur. J.*, 2008, **14**, 7670–7679.
25 Ö. Göktuğ, C. Göl and M. Durmuş, *J. Porphyrins phthalocyanines*, 2017, **21**, 539–546.
26 F. Ma, G. Zhang, X. Wu, W. Qu, Z. Sun, X. Li and X. Yin, *J. Phys. Chem. C*, 2022, **126**, 13496–13504.